

Buckling of symmetrically laminated quasi-isotropic thin rectangular plates

Erkin Altunsaray ^{*1} and İsmail Bayer ²

¹ *Institute of Marine Science and Technology, Dokuz Eylul University,
Baku Bulvari, 100, TR-35340, Izmir, Turkey*

² *Department of Naval Architecture and Marine Engineering, Yildiz Technical University,
TR-34349 Besiktas, Istanbul, Turkey*

(Received October 31, 2013, Revised February 17, 2014, Accepted March 23, 2014)

Abstract. The lowest critical value of the compressive force acting in the plane of symmetrically laminated quasi-isotropic thin rectangular plates is investigated. The critical buckling loads of plates with different types of lamination and aspect ratios are parametrically calculated. Finite Differences Method (FDM) and Galerkin Method are used to solve the governing differential equation for Classical Laminated Plate Theory (CLPT). The results calculated are compared with those obtained by the software ANSYS employing Finite Elements Method (FEM). The results of Galerkin Method (GM) are closer to FEM results than those of FDM. In this study, the primary aim is to conduct a parametrical performance analysis of proper plates that is typically conducted at preliminary structural design stage of composite vessels. Non-dimensional values of critical buckling loads are also provided for practical use for designers.

Keywords: critical buckling load; finite differences method; the Galerkin method; parametric study; symmetrically laminated quasi-isotropic plates

1. Introduction

Composite materials are currently being used in many engineering structures. They are increasingly preferred in naval architecture due to the progress being made in both the specific materials being used and novel production technologies. They have superior mechanical properties such as high specific strength and high specific rigidity, while offering freedom for particular design requirements by allowing the adjustment of their chemical components and orientation angles (Reuben 1994). There are several applications of composites in marine engineering (Shenoi and Wellicome 1993a, b). Mouritz *et al.* (2001) showed the application of composite materials to submarines and navy ships.

Ships are formed by plates and shells whose thickness is relatively small in comparison to other dimensions like the length and width and are stiffened by structural elements using beams and/or girders. A ship moving through waves is likely to bend longitudinally depending on the loading conditions, which means that the ship will alternately sag or hog. When the ship is in a sagging

*Corresponding author, Ph.D., E-mail: erkin.altunsaray@deu.edu.tr

condition, the deck must resist compressive loads. In hogging conditions the bottom is under axial compressive loads. Deck, side and bottom plating of ships are supported by longitudinal and transversal stiffeners or girders that may be considered as thin plates. Therefore, it is reasonable to use Classical Laminated Plate Theory (CLPT) for the buckling analysis of orthotropic plates, which is presented by Reddy (2004). Szilard (2004) calculated the critical buckling loads of isotropic and orthotropic rectangular plates under the effect of in plane forces using the Galerkin Method and the Finite Differences Method (FDM).

Due to the current restrictions in production of composite marine structures, composite materials composed of thermosetting resin and laminates generally use orientation angles of 0° , 90° , 45° and -45° . The structure is referred to as a symmetrical laminate, provided that laminates at both side of the mid plane of symmetry and are of equal distance from the mid plane, and further that they have the same orientation angle. Symmetrically laminated structures are preferred in practice, since they do not have any distortions during the cooling stage after the hot curing process (ASM Handbook 2001, Powell 1994, Mallick 1997).

Darvizeh and Darvizeh (2002) examined buckling analysis of orthotropic composite plates for different boundary conditions using the Differential Quadrature Method (DQM) and the Finite Element Method (FEM). Hu *et al.* (2003) focused on buckling of a symmetrically laminated rectangular plate subject to parabolic variation of axial loads using the Rayleigh–Ritz method. Buckling load values were obtained based on CLPT. They performed stability analysis for composite plates with laminate configurations of $[0^\circ, 0^\circ]$, $[0^\circ, \pm 15^\circ]$, $[0^\circ, \pm 30^\circ]$, $[0^\circ, \pm 45^\circ]$, $[0^\circ, \pm 60^\circ]$, $[0^\circ, \pm 75^\circ]$, $[0^\circ, \pm 90^\circ]$. Baltaci *et al.* (2007) carried out buckling analysis of composite circular plates based on CLPT and the First Order Shear Deformation Theory (FSDT) using FEM. They examined $[\pm 45^\circ]_{2s}$, $[\pm 45^\circ, \pm 45^\circ]_{2s}$, $[90^\circ/0^\circ_2/90^\circ]_s$, $[90^\circ/0^\circ]_{2s}$, $[90^\circ/0^\circ]_4$, $[90^\circ/0^\circ_2/90^\circ]_2$, $[\pm 45^\circ, \pm 45^\circ]_{2s}$, $[\pm 45^\circ]_4$ laminated plate types. Özben (2009) calculated analytically critical buckling load values of composite plates with different boundary conditions as well as using FEM. In his research critical buckling load values of symmetrical and anti-symmetrical composite plates were obtained for various plate edge ratio and fiber orientation angles. He calculated critical buckling load of composite plates with lamination angles of $[0^\circ/0^\circ]$, $[0^\circ/15^\circ]$, $[0^\circ/30^\circ]$, $[0^\circ/45^\circ]$. Panda and Ramachandra (2010) examined non-dimensional buckling load coefficients of rectangular composite plates under parabolic compression for different edge conditions using the Galerkin Method and FEM. They examined cross-ply plates $[0^\circ/90^\circ/0^\circ]$. Felix *et al.* (2011) investigated the buckling and vibration of a clamped orthotropic rectangular thin plate subject to a linearly varying in-plane load using the Ritz method and FEM. Rajasekaran and Wilson (2013) studied buckling and vibration of rectangular isotropic plates with various boundary conditions by using the finite difference technique. Recently, Altunsaray and Bayer (2013) investigated the deflection and free vibration of symmetrically laminated quasi-isotropic thin rectangular plates for different boundary conditions based on CLPT using the Galerkin Method, the Least Square Method and FEM.

It would appear that critical buckling load values of symmetrically and anti-symmetrically laminated orthotropic composite plates and cross-ply plates with different shapes and boundary conditions has been sufficiently well investigated by using a number of different numerical methods. Although Galerkin Method, FDM and FEM are quite well known numerical methods used for the solution of engineering problems, to the best knowledge of the authors, there have not been many attempts to use these methods for the buckling of quasi-isotropic thin rectangular plates laminated with some combinations of orientation angles of 0° , -45° , 45° and 90° , for different aspect ratios. Therefore, in this particular study, it is intended to present the comparison of the

Galerkin Method, FDM and FEM for analysis of the critical buckling loads of symmetrically laminated quasi-isotropic thin rectangular plates with all edges simply supported. Fourteen different types of lamination (0° , -45° , 45° and 90°) quasi-isotropic plates are obtained for the critical buckling load as well as the non-dimensional critical buckling load so that they may be used practically for designers at the preliminary design stage. The main reason for considering only those fourteen lamination types out of total twenty four possibilities is that the critical buckling load values obtained by all the three methods employed are close and consistent.

The plates laminated with orientation angles of 0° , 90° , 45° and -45° are under the effect of compressive load (N_x) through x axis (Fig. 1). The structure of a ship is referred to either longitudinally framed or laterally framed depending on the configuration of stiffeners. The critical buckling loads are parametrically calculated by considering the short edge of plates (b) is at x axis or y axis, in order to represent the longitudinal or lateral framing system of a ship, for 6 different aspect ratios and for 14 different types of lamination. Finite Differences Method (FDM) and Galerkin Method are used to solve the governing differential equation for Classical Laminated Plate Theory (CLPT). The results calculated are compared with those obtained by the software ANSYS employing Finite Elements Method (FEM). The results of Galerkin Method are closer to FEM results than FDM results.

2. Material and method

2.1 Geometry of plates, material properties and lamination types

The geometry of the plate is shown in Fig. 1. Aspect ratios used in parametrical analyses are given below in Table 1. Material properties of T300-934 carbon/epoxy (ides The Plastic Web 2013, About.com Composite / Plastic 2013) selected for this study are given in Table 2.

Fourteen different types of lamination of quasi-isotropic plates considered in this study are shown in Table 3. The thickness of each laminate (t) is equal to 0.0002 meter and the thickness of the plate formed by 16 laminates (h) is equal to 0.0032 meter.

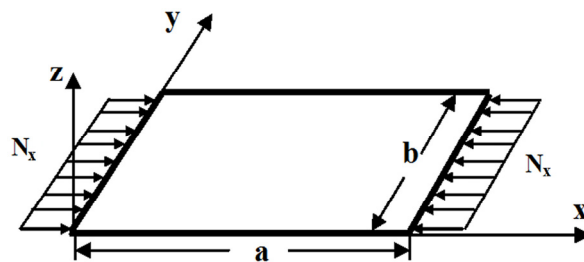


Fig. 1 Plate Geometry

Table 1 Aspect ratios

		Aspect ratios				
a/b	1	1.2	1.4	1.6	1.8	2
b/a	1	1.2	1.4	1.6	1.8	2

Table 2 Material properties of T300-934 carbon/epoxy (ides The Plastic Web 2013, About.com Composite / Plastic 2013)

Longitudinal young modulus (E_{11})	148×10^9 (N/m ²)
Transversal young modulus (E_{22})	9.65×10^9 (N/m ²)
Longitudinal shear modulus (G_{12})	4.55×10^9 (N/m ²)
Longitudinal poisson ratio (ν_{12})	0.30
Laminate thickness (t)	$0.185 \times 10^{-3} - 0.213 \times 10^{-3}$ (m)

Table 3 Symmetrically laminated quasi-isotropic plate types

LT1	$[-45_2/45_2/0_2/90_2]_s$	LT8	$[45_2/-45_2/0_2/90_2]_s$
LT2	$[-45_2/45_2/90_2/0_2]_s$	LT9	$[45_2/-45_2/90_2/0_2]_s$
LT3	$[0_2/-45_2/45_2/90_2]_s$	LT10	$[90_2/-45_2/0_2/45_2]_s$
LT4	$[0_2/-45_2/90_2/45_2]_s$	LT11	$[90_2/-45_2/45_2/0_2]_s$
LT5	$[0_2/45_2/-45_2/90_2]_s$	LT12	$[90_2/0_2/45_2/-45_2]_s$
LT6	$[0_2/45_2/90_2/-45_2]_s$	LT13	$[90_2/45_2/-45_2/0_2]_s$
LT7	$[0_2/90_2/-45_2/45_2]_s$	LT14	$[90_2/45_2/0_2/-45_2]_s$

2.2 Classical Laminated Plate Theory (CLPT)

According to the Classical Laminated Plate Theory, because the bending-strain coupling matrix of symmetrically laminated plates B_{ij} is zero, the governing differential equation of the symmetrically laminated composite plates under the effect of uniform axial load on x axis may be given as follows, Eq. (1) (Reddy 2004).

$$\left(D_{11} \frac{\partial^4 w}{\partial x^4} + 4D_{16} \frac{\partial^4 w}{\partial x^3 \partial y} + 2(D_{12} + 2D_{66}) \frac{\partial^4 w}{\partial x^2 \partial y^2} + 4D_{26} \frac{\partial^4 w}{\partial x \partial y^3} + D_{22} \frac{\partial^4 w}{\partial y^4} \right) - N_x \left(\frac{\partial^4 w}{\partial x^4} \right) = 0 \quad (1)$$

In the above Eq. (1) “ w ” represents the deflection function, while “ N_x ” represents the uniform axial load. The bending stiffness matrix elements D_{11} , D_{12} , D_{16} , D_{22} , D_{26} and D_{66} are calculated as shown below (Reddy 2004).

$$D_{ij} = \frac{1}{3} \sum_{k=1}^N \bar{Q}_{ij}^{(k)} (z_{k+1}^3 - z_k^3) \quad (2)$$

As shown below in Eq. (3), the elements of the \bar{Q}_{ij} transformed reduced stiffness matrix in the above equation are calculated separately for each lamina by utilizing the Q_{ij} reduced stiffness matrix elements and the θ angle each lamina makes with the principal axis (Reddy 2004).

$$\begin{aligned} \bar{Q}_{11} &= Q_{11} \cos^4(\theta) + 2(Q_{12} + 2Q_{66}) \sin^2(\theta) \cos^2(\theta) + Q_{22} \sin^4(\theta) \\ \downarrow \bar{Q}_{12} &= (Q_{11} + Q_{22} - 4Q_{66}) \sin^2(\theta) \cos^2(\theta) + Q_{12} (\sin^4(\theta) + \cos^4(\theta)) \end{aligned} \quad (3)$$

$$\begin{aligned}
\uparrow \bar{Q}_{22} &= Q_{11} \sin^4(\theta) + 2(Q_{12} + 2Q_{66})\sin^2(\theta)\cos^2(\theta) + Q_{22}\cos^4(\theta) \\
\bar{Q}_{16} &= (Q_{11} - Q_{12} - 2Q_{66})\sin(\theta)\cos^3(\theta) + (Q_{12} - Q_{22} + 2Q_{66})\sin^3(\theta)\cos(\theta) \\
\bar{Q}_{26} &= (Q_{11} - Q_{12} - 2Q_{66})\sin^3(\theta)\cos(\theta) + (Q_{12} - Q_{22} + 2Q_{66})\sin(\theta)\cos^3(\theta) \\
\bar{Q}_{66} &= (Q_{11} + Q_{22} - 2Q_{12} - 2Q_{66})\sin^2(\theta)\cos^2(\theta) + Q_{66}(\sin^4(\theta) + \cos^4(\theta))
\end{aligned} \quad (3)$$

For orthotropic materials, the notation of the elements of the Q_{ij} reduced stiffness matrix in the above equation in terms of engineering constants is given below (Reddy 2004).

$$\begin{aligned}
Q_{11} &= E_{11}/(1 - \nu_{12}\nu_{21}) \\
Q_{12} &= \nu_{12}E_{22}/(1 - \nu_{12}\nu_{21}) \\
Q_{22} &= E_{22}/(1 - \nu_{12}\nu_{21}) \\
Q_{66} &= G_{12}
\end{aligned} \quad (4)$$

By substituting the engineering constants (E , G and ν), the angles of the laminas and the distance of each lamina from the reference plane into the relative places in the Eqs. (2)-(3)-(4), the bending stiffness matrix elements D_{ij} in Eq. (1) are determined.

In the case of simply supported edges, deflection and bending moment along the edges of the plate are zero.

$$\begin{aligned}
w = M_x = 0 \quad \text{at} \quad x = 0 \quad \text{and} \quad x = a \\
w = M_y = 0 \quad \text{at} \quad y = 0 \quad \text{and} \quad y = b
\end{aligned} \quad (5)$$

2.3 The Galerkin method

In the Galerkin Method, solution is found by evanishing the integral of the multiplication of the error function (ε_R) with the ϕ_i terms of the coordinate (approach) function preselected for the solution of the problem. It is known as a highly robust method among the weighted residual methods (Reddy 2004).

$$\int_{\Omega} \varepsilon_R \phi_i d\Omega = 0, \quad i = 1, 2, \dots, n \quad (6)$$

2.4 Application of the Galerkin method

The differential equation used for the buckling of symmetrically laminated composite plates is given in Eq. (1) under the Section 2.2. In the Eq. (1), “ w ” indicates the deflection function, while N_x represents uniform axial compressive load. The bending stiffness matrix elements D_{ij} are as shown in Section 2.2.

The approach function satisfying the boundary conditions for simply supported edges given in Eq. (5) is shown below.

$$\varphi_i \varphi_j = \sin\left(\frac{i\pi x}{a}\right) \sin\left(\frac{j\pi y}{b}\right) \quad (i = 1, \dots, m; j = 1, \dots, n) \quad (7)$$

The approximate deflection function (w_0) may be chosen as the multiplication of the approach

function with the unknown constants (c_i). Only the first term of the deflection function ($i = j = 1$) is used for calculations.

$$w_0 = c_i \varphi_i \varphi_j \tag{8}$$

In order to determine the critical buckling value (N_x), the error function (ε_R) obtained by substituting the approximate deflection function into the governing differential equation Eq. (1) is multiplied with the selected approach function and its integral is vanished.

$$\int_0^b \int_0^a \left(\begin{aligned} & D_{11} \frac{\partial^4 w_{mn}}{\partial x^4} + 4D_{16} \frac{\partial^4 w_{mn}}{\partial x^3 \partial y} + 2(D_{12} + 2D_{66}) \frac{\partial^4 w_{mn}}{\partial x^2 \partial y^2} \\ & + 4D_{26} \frac{\partial^4 w_{mn}}{\partial x \partial y^3} + D_{22} \left(\frac{\partial^4 w_{mn}}{\partial y^4} \right) - N_x \left(\frac{\partial^2 w_{mn}}{\partial x^2} \right) \end{aligned} \right) \varphi_i \varphi_j d_x d_y = 0 \tag{9}$$

where m and n indicate mode shapes and they were taken to be one ($m = n = 1$) for calculations. It is a simple eigenvalue problem and the critical buckling load (N_x) is found.

2.5 Finite differences method

Finite Differences Method, one of the numerical methods for approximate solutions, transforms the governing differential equation into algebraic equations by finite differences schemes. Variations in two directions exist for the plate differential equation (Szilard 2004).

In this study, intervals between pivotal points in x and y directions (Δx and Δy) are taken to be $a/3$ and $b/3$ respectively as shown in Fig. 2. The governing differential equation for symmetrically laminated plates subjected to axial uniform compressive load in x direction was already given Eq. (1).

The boundary conditions for simply supported edges were given by Eq. (5). In order to satisfy the boundary conditions, the values of w at pivotal points immediately outside the boundary are taken to be equal to the negative values of w at points immediately inside the boundary.

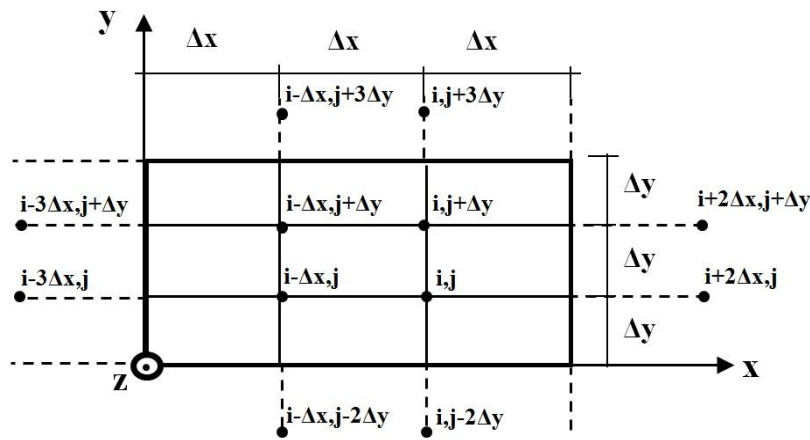


Fig. 2 Finite differences grid

$$\begin{aligned}
w_{i,j} &= -w_{i+2\Delta x,j} = -w_{i,j-2\Delta y} \\
w_{i,j+\Delta y} &= -w_{i+2\Delta x,j} = -w_{i,j+3\Delta y} \\
w_{i-\Delta x,y} &= -w_{i-3\Delta x,j} = -w_{i-\Delta x,y+3\Delta y} \\
w_{i-\Delta x,y} &= -w_{i-3\Delta x,j} = -w_{i-\Delta x,y-2\Delta y}
\end{aligned} \tag{10}$$

The following central differences operators are used to obtain a finite difference scheme for the governing differential equation (Saracoglu and Özelikörs 2011).

$$\frac{\partial^2 w}{\partial x^2} \approx \frac{w_{i+\Delta x,y} - 2w_{i,y} + w_{i-\Delta x,y}}{(\Delta x)^2} \tag{11a}$$

$$\frac{\partial^3 w}{\partial x^3} \approx \frac{w_{i+2\Delta x,y} - 2w_{i+\Delta x,y} + 2w_{i-\Delta x,y} - w_{i-2\Delta x,y}}{2(\Delta x)^3} \tag{11b}$$

$$\frac{\partial^4 w}{\partial x^4} \approx \frac{w_{i+2\Delta x,y} - 4w_{i+\Delta x,y} + 6w_{i,j} - 4w_{i-\Delta x,y} + w_{i-2\Delta x,y}}{(\Delta x)^4} \tag{11c}$$

$$\frac{\partial^2 w}{\partial y^2} \approx \frac{w_{i,j+\Delta y} - 2w_{i,y} + w_{i,j-\Delta y}}{(\Delta y)^2} \tag{11d}$$

$$\frac{\partial^3 w}{\partial y^3} \approx \frac{w_{i,j+2\Delta y} - 2w_{i,j+\Delta y} + 2w_{i,j-\Delta y} - w_{i,j-2\Delta y}}{2(\Delta y)^3} \tag{11e}$$

$$\frac{\partial^4 w}{\partial y^4} \approx \frac{w_{i,j+2\Delta y} - 4w_{i,j+\Delta y} + 6w_{i,j} - 4w_{i,j-\Delta y} + w_{i,j-2\Delta y}}{(\Delta y)^4} \tag{11f}$$

$$\frac{\partial^2 w}{\partial x \partial y} \approx \frac{w_{i+\Delta x,y+\Delta y} - w_{i-\Delta x,y+\Delta y} - w_{i+\Delta x,y-\Delta y} + w_{i-\Delta x,y-\Delta y}}{4(\Delta x)(\Delta y)} \tag{11g}$$

$$\frac{\partial^3 w}{\partial x \partial y^2} \approx \frac{w_{i+\Delta x,y+\Delta y} - 2w_{i,j+\Delta y} + w_{i-\Delta x,y+\Delta y}}{2(\Delta y)(\Delta x)^2} + \frac{-w_{i+\Delta x,y-\Delta y} + 2w_{i,j-\Delta y} - w_{i-\Delta x,y-\Delta y}}{2(\Delta y)(\Delta x)^2} \tag{11h}$$

$$\begin{aligned}
\frac{\partial^4 w}{\partial x \partial y^3} &\approx \frac{w_{i+2\Delta x,y+\Delta y} - w_{i+2\Delta x,y-\Delta y} - 2w_{i+\Delta x,y+\Delta y} + 2w_{i+\Delta x,y-2\Delta y}}{4(\Delta x)^3(\Delta y)} \\
&+ \frac{2w_{i-\Delta x,y+\Delta y} - 2w_{i-\Delta x,y-\Delta y} - w_{i-2\Delta x,y+\Delta y} - w_{i-2\Delta x,y-\Delta y}}{4(\Delta x)^3(\Delta y)}
\end{aligned} \tag{11i}$$

$$\frac{\partial^3 w}{\partial x \partial y^2} \approx \frac{w_{i+\Delta x, y+\Delta y} - 2w_{i+\Delta x, y} + w_{i+\Delta x, y-\Delta y} - w_{i-\Delta x, y+\Delta y}}{2(\Delta x)(\Delta y)^2} + \frac{2w_{i-\Delta x, y} - w_{i-\Delta x, y-\Delta y}}{2(\Delta x)(\Delta y)^2} \quad (11j)$$

$$\begin{aligned} \frac{\partial^4 w}{\partial x \partial y^3} \approx & \frac{w_{i+\Delta x, y+2\Delta y} - 2w_{i+\Delta x, y+\Delta y} + 2w_{i+\Delta x, y-\Delta y} - w_{i+\Delta x, y-2\Delta y}}{4(\Delta y)^3(\Delta x)} \\ & + \frac{-w_{i-\Delta x, y+2\Delta y} + 2w_{i-\Delta x, y+\Delta y} - 2w_{i-\Delta x, y-\Delta y} + w_{i-\Delta x, y-2\Delta y}}{4(\Delta x)^3(\Delta y)} \end{aligned} \quad (11k)$$

$$\begin{aligned} \frac{\partial^4 w}{\partial y^2 \partial x^2} \approx & \frac{w_{i+\Delta x, y+\Delta y} - 2w_{i, j+\Delta y} + w_{i-\Delta x, y+\Delta y} - 2w_{i+\Delta x, y} + 4w_{i, j}}{(\Delta x)^2(\Delta y)^2} \\ & + \frac{-2w_{i-\Delta x, y} + w_{i-\Delta x, y-\Delta y} - 2w_{i, j-\Delta y} + w_{i-\Delta x, y-\Delta y}}{(\Delta x)^2(\Delta y)^2} \end{aligned} \quad (11l)$$

This is an eigenvalue problem and the critical buckling loads are calculated by substituting the above operators into Eq. (1).

2.6 Finite Elements Method (FEM) software package ANSYS

ANSYS software package employing Finite Elements Method (FEM) is run to check the results obtained by Galerkin Method and FDM. Shell element (SHELL 181) with four nodal points proposed by the software package is used. The ratio of the length of the short edge of the plate to the length of the nodal element is taken to be 20 for converging results.

3. Results of parametric analyses

In this section, using the parameters given in Section 2.1, the critical buckling loads of simply supported composite rectangular plates, which are found by GM and FDM, are presented to be compared with the results of ANSYS software. The effect of change in aspect ratio and orientation angle is shown in Fig. 3 and Table 4, when the short edge of plate is at y axis. The corresponding results, when the short edge of plate is at x axis, are given in Fig. 4 and Table 5.

- It can be noticed from Tables 4-5 that the critical buckling loads of LT1, LT2, LT3, LT4, LT10 and LT11 coincide with LT8, LT9, LT5, LT6, LT14 and LT13 respectively. When the short edge is on the y axis, which corresponds to ‘longitudinal framing system’, the critical buckling loads increase in general, as the aspect ratio (a/b) increases. On the other hand, when the short edge is on the x axis, which corresponds to ‘lateral framing system’, the critical buckling loads decrease in general, as the aspect ratio (b/a) increases. This finding is consistent with the critical buckling load results of isotropic rectangular plates. The highest critical buckling load is reached with lamination type LT11 and LT13, when the short edge of plate is at y axis and the aspect ratio is equal to 2. The highest critical buckling load is reached with lamination type LT3 and LT5, when the short edge of plate is at x axis and the aspect ratio is equal to 2. It can be seen that the GM results are closer to FEM results than FDM results.

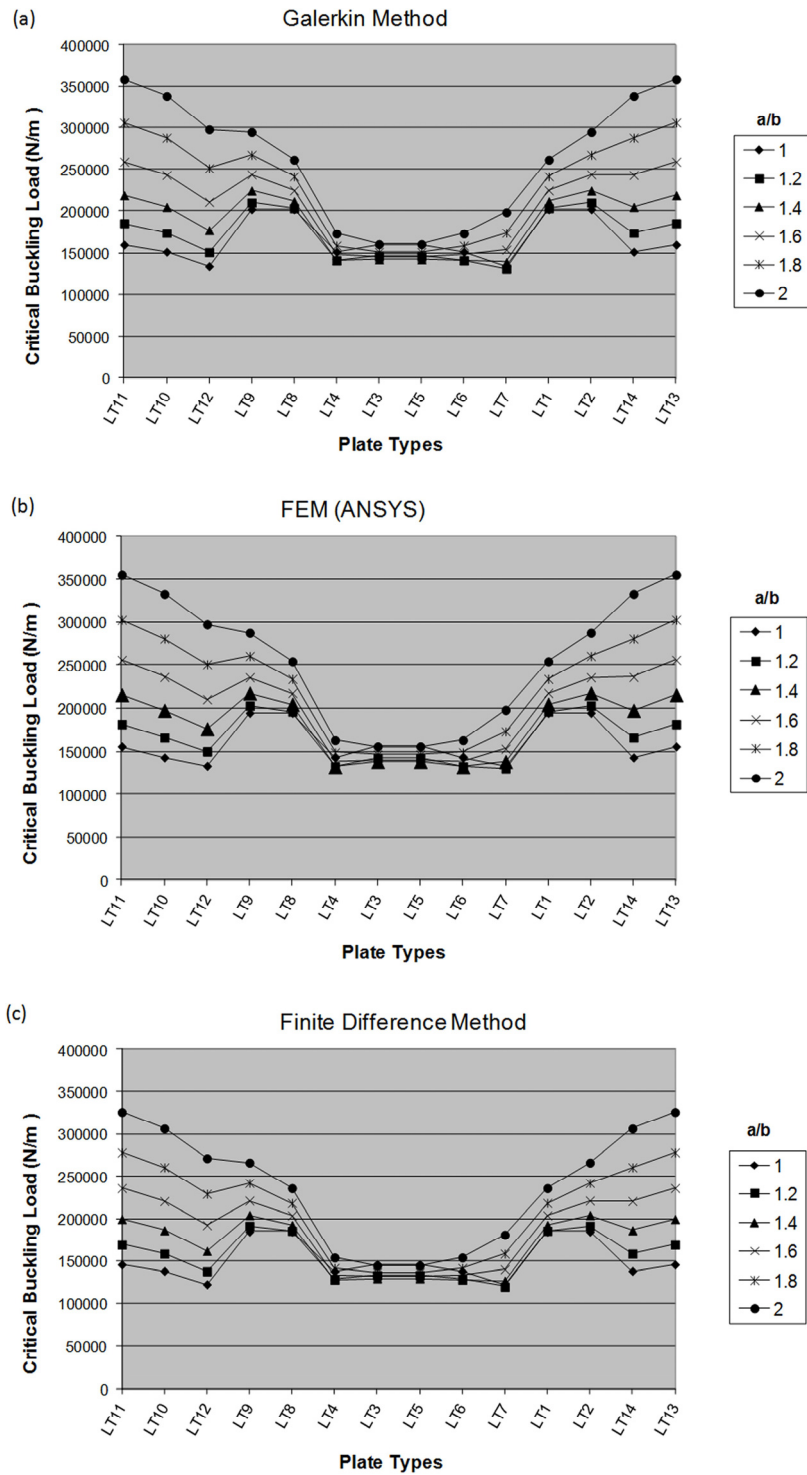


Fig. 3 Critical buckling load (N/m), short edge is on the y axis: (a) Galerkin Method; (b) Finite Elements Method (FEM); (c) Finite Differences Method (FDM)

- When a second term is included in the approximate deflection function, the results of GM did not change significantly. When the interval between pivotal points is reduced, the results of FDM did not improve significantly, either. However, it is interesting to see that the GM results are upper bound, while the FDM results are a lower bound, as expected.
- The critical buckling loads calculated by GM for carbon/epoxy, whose material properties are given in Section 2.1, are presented in non-dimensional form as a function of plate short edge (b or a), laminate thickness (t) and transversal Young modulus (E_{22}) in Table 6. Provided that the unit of length is meter, the non-dimensional values are given as $N_0^* = N_x \frac{b^2}{t^3 E_{22}}$, when the short edge of plate is 'b', as $N_0^* = N_x \frac{a^2}{t^3 E_{22}}$, when the short edge of plate is 'a'. A number of parameters are taken into account in production of composite vessels. Savings of time, material, manpower and cost may be gained at the preliminary design stage of such vessels by providing tables of non-dimensional buckling loads obtained by parametrical analyses to determine the most proper plate configuration.
- It is unfortunate that the findings are not compared with those published in the literature, because the authors were unable to find any results obtained by similar methods for this particular problem dealt with.

Table 4 Critical buckling load (N/m), short edge is on the y axis

a/b	Method	Plate types						
		LT1	LT2	LT3	LT4	LT5	LT6	LT7
		N_x (N/m)	N_x (N/m)	N_x (N/m)	N_x (N/m)	N_x (N/m)	N_x (N/m)	N_x (N/m)
1	Galerkin	202359.7	202359.7	159863.1	151363.8	159863.1	151363.8	134365.1
	FDM	184529.9	184529.9	145777.6	138027.2	145777.6	138027.2	122526.3
	FEM (ANSYS)	194881.0	194846.0	155872.0	143071.0	155872.0	143071.0	133201.0
1.2	Galerkin	203598.9	210152.7	146146.1	141209.4	146146.1	141209.4	131335.9
	FDM	185450.7	191433.6	133139.7	128466.0	133139.7	128466.0	119727.9
	FEM (ANSYS)	196319.0	202943.0	142074.0	132454.0	142074.0	132454.0	130296.0
1.4	Galerkin	211782.2	224526.7	142419.9	141292.0	142419.9	141292.0	139036.0
	FDM	192419.5	204080.8	129407.0	127791.9	129407.0	127791.9	126666.5
	FEM (ANSYS)	204540.0	217460.0	138197.0	132108.0	138197.0	132108.0	138107.0
1.6	Galerkin	224757.4	243827.4	144685.5	147741.1	144685.5	147741.1	153852.2
	FDM	203617.4	221111.0	131014.7	132698.6	131014.7	132698.6	140078.9
	FEM (ANSYS)	217461.0	235507.0	140297.0	138196.0	140297.0	138196.0	153036.0
1.8	Galerkin	241496.5	267264.6	151032.4	158707.8	151032.4	158707.8	174058.5
	FDM	218194.2	241885.6	136287.5	141662.4	136287.5	141662.4	158409.2
	FEM (ANSYS)	233730.0	260340.0	146487.0	148857.0	146487.0	148857.0	173360.0
2	Galerkin	261457.8	294422.3	160454.4	173218.2	160454.4	173218.2	198745.7
	FDM	235707.6	266068.5	144353.8	153889.5	144353.8	153889.5	180835.9
	FEM (ANSYS)	254141.0	287457.0	155766.0	163065.0	155766.0	163065.0	198175.0

Table 4 Continued

a/b	Method	Plate types						
		LT8	LT9	LT10	LT11	LT12	LT13	LT14
		N_x (N/m)	N_x (N/m)	N_x (N/m)	N_x (N/m)	N_x (N/m)	N_x (N/m)	N_x (N/m)
1	Galerkin	202359.7	202359.7	151363.8	159863.1	134365.1	159863.1	151363.8
	FDM	184529.9	184529.9	138027.2	145777.6	122526.3	145777.6	138027.2
	FEM (ANSYS)	194881.0	194846.0	142903.0	155762.0	133193.0	155762.0	142903.0
1.2	Galerkin	203598.9	210152.7	173978.5	185469.1	150997.4	185469.1	173978.5
	FDM	185450.7	191433.6	158404.5	169025.4	137661.7	169025.4	158404.5
	FEM (ANSYS)	196319.0	202943.0	166155.0	181732.0	149996.0	181732.0	166155.0
1.4	Galerkin	211782.2	224526.7	205014.3	218886.8	177269.4	218886.8	205014.3
	FDM	192419.5	204080.8	186224.8	199298.3	161556.9	199298.3	186224.8
	FEM (ANSYS)	204540.0	217460.0	197620.0	215415.0	176426.0	215415.0	197620.0
1.6	Galerkin	224757.4	243827.4	243090.8	259105.2	211062.1	259105.2	243090.8
	FDM	203617.4	221111.0	220435.7	235759.1	192306.9	235759.1	220435.7
	FEM (ANSYS)	217461.0	235507.0	235945.0	255828.0	210368.0	255828.0	235945.0
1.8	Galerkin	241496.5	267264.6	287548.7	305641.5	251363.1	305641.5	287548.7
	FDM	218194.2	241885.6	260510.7	277998.5	228998.7	277998.5	260510.7
	FEM (ANSYS)	233730.0	260340.0	280554.0	302473.0	250814.0	302473.0	280554.0
2	Galerkin	261457.8	294422.3	338040.5	358241.2	297639.2	358241.2	338040.5
	FDM	235707.6	266068.5	306152.6	325792.9	271148.2	325792.9	306152.6
	FEM (ANSYS)	254141.0	287457.0	332835.0	355136.0	297233.0	355136.0	332835.0

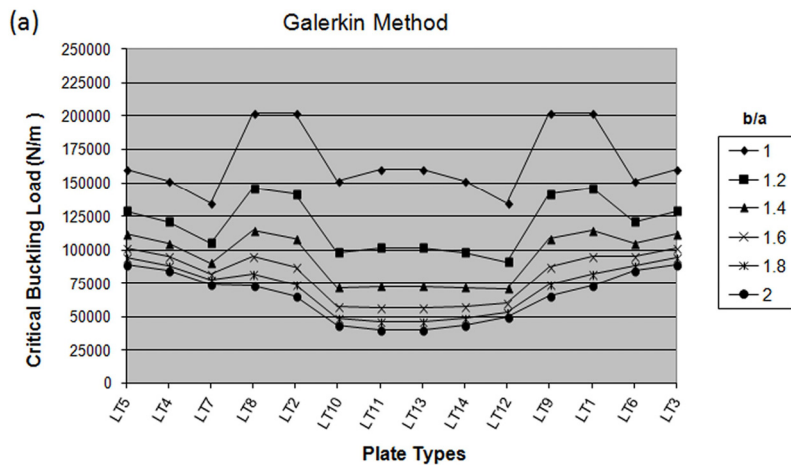


Fig. 4 Critical buckling load (N/m), short edge is on the x axis: (a) Galerkin Method; (b) Finite Elements Method (FEM); (c) Finite Differences Method (FDM)

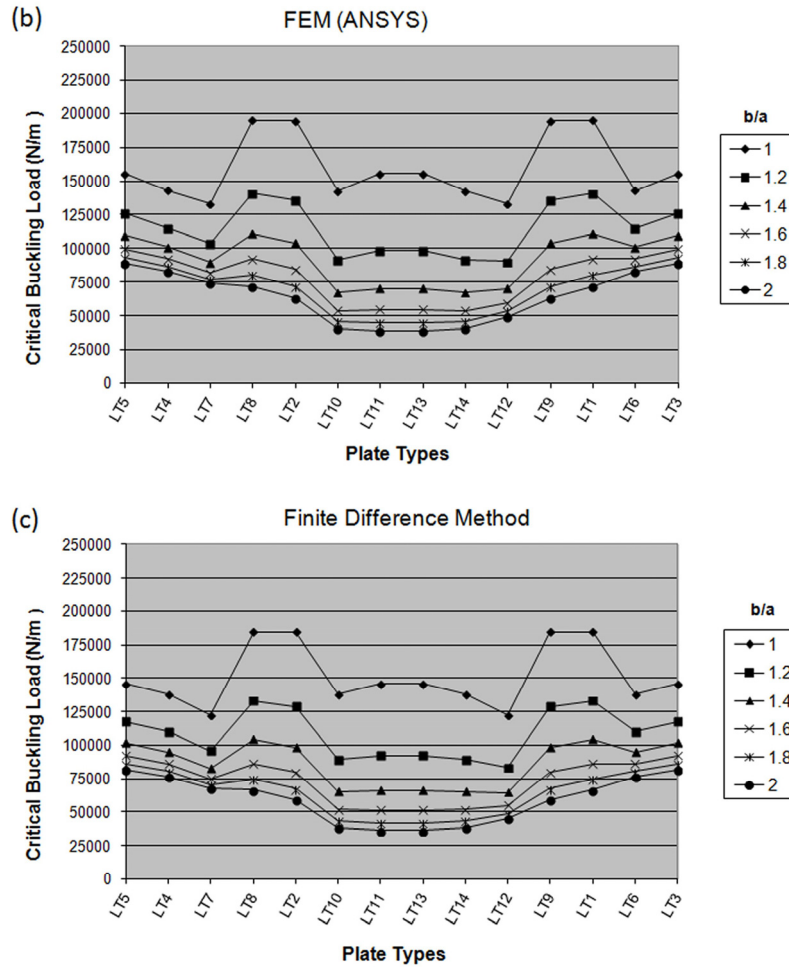


Fig. 4 Continued

Table 5 Critical buckling load (N/m), short edge is on the x axis

b/a	Method	Plate types						
		LT1	LT2	LT3	LT4	LT5	LT6	LT7
		N_x (N/m)	N_x (N/m)	N_x (N/m)	N_x (N/m)	N_x (N/m)	N_x (N/m)	N_x (N/m)
1	Galerkin	202359.7	202359.7	159863.1	151363.8	159863.1	151363.8	134365.1
	FDM	184529.9	184529.9	145777.6	138027.2	145777.6	138027.2	122526.3
	FEM (ANSYS)	194881.0	194846.0	155872.0	143071.0	155872.0	143071.0	133201.0
1.2	Galerkin	145939.4	141388.1	128798.0	120818.4	128798.0	120818.4	104859.3
	FDM	132940.0	128785.2	117378.7	110003.2	117378.7	110003.2	95598.4
	FEM (ANSYS)	140813.5	136169.3	126159.6	115437.3	126159.6	115437.3	104043.8

Table 5 Continued

<i>b/a</i>	Method	Plate types						
		LT1	LT2	LT3	LT4	LT5	LT6	LT7
		N_x (N/m)	N_x (N/m)	N_x (N/m)	N_x (N/m)	N_x (N/m)	N_x (N/m)	N_x (N/m)
1.4	Galerkin	114554.4	108052.1	111676.9	104599.1	111676.9	104599.1	90443.6
	FDM	104122.9	98173.2	101682.8	95012.6	101682.8	95012.6	82427.0
	FEM (ANSYS)	110796.8	104177.5	109802.3	100847.0	109802.3	100847.0	89846.5
1.6	Galerkin	95245.1	87795.9	101213.0	94957.4	101213.0	94957.4	82446.1
	FDM	86371.5	79538.0	92093.4	86107.7	92093.4	86107.7	75119.9
	FEM (ANSYS)	92355.4	84782.1	99804.9	92192.0	99804.9	92192.0	81987.4
1.8	Galerkin	82489.1	74535.9	94333.8	88749.6	94333.8	88749.6	77581.2
	FDM	74656.1	67343.9	85802.0	80404.5	85802.0	80404.5	70678.6
	FEM (ANSYS)	80187.3	72111.9	93229.5	86622.0	93229.5	86622.0	77213.8
2	Galerkin	73605.6	65364.5	89560.3	84510.1	89560.3	84510.1	74409.8
	FDM	66517.1	58926.9	81448.2	76538.2	81448.2	76538.2	67787.0
	FEM (ANSYS)	71722.6	63365.4	88664.1	82816.7	88664.1	82816.7	74105.1

<i>b/a</i>	Method	Plate types						
		LT8	LT9	LT10	LT11	LT12	LT13	LT14
		N_x (N/m)	N_x (N/m)	N_x (N/m)	N_x (N/m)	N_x (N/m)	N_x (N/m)	N_x (N/m)
1	Galerkin	202359.7	202359.7	151363.8	159863.1	134365.1	159863.1	151363.8
	FDM	184529.9	184529.9	138027.2	145777.6	122526.3	145777.6	138027.2
	FEM (ANSYS)	194881.0	194846.0	142903.0	155762.0	133193.0	155762.0	142903.0
1.2	Galerkin	145939.4	141388.1	98062.1	101490.4	91205.5	101490.4	98062.1
	FDM	132940.0	128785.2	89212.5	92458.1	83144.4	92458.1	89212.5
	FEM (ANSYS)	140813.5	136169.3	91802.7	98488.6	90368.2	98488.6	91802.7
1.4	Galerkin	114554.4	108052.1	72087.7	72663.2	70936.7	72663.2	72087.7
	FDM	104122.9	98173.2	65199.9	66024.0	64625.8	66024.0	65199.9
	FEM (ANSYS)	110796.8	104177.5	67249.8	70343.3	70322.8	70343.3	67249.8
1.6	Galerkin	95245.1	87795.9	57711.4	56517.8	60098.5	56517.8	57711.4
	FDM	86371.5	79538.0	51835.4	51177.6	54718.3	51177.6	51835.4
	FEM (ANSYS)	92355.4	84782.1	53859.7	54657.8	59634.3	54657.8	53859.7
1.8	Galerkin	82489.1	74535.9	48983.9	46614.9	53721.8	46614.9	48983.9
	FDM	74656.1	67343.9	43723.0	42064.0	48891.7	42064.0	43723.0
	FEM (ANSYS)	80187.3	72111.9	45848.6	45085.0	53360.7	45085.0	45848.6
2	Galerkin	73605.6	65364.5	43304.5	40113.6	49686.4	40113.6	43304.5
	FDM	66517.1	58926.9	38472.4	36088.4	45209.0	36088.4	38472.4
	FEM (ANSYS)	71722.6	63365.4	40706.5	38831.1	49398.5	38831.1	40706.5

Table 6 Non-dimensional critical buckling load ($N_0^* = N_x \frac{b^2}{t^3 E_{22}}$ for a/b , $N_0^* = N_x \frac{a^2}{t^3 E_{22}}$ for b/a)

Plate type	Aspect ratio					
	a/b					
	1	1.2	1.4	1.6	1.8	2
LT1	104855	105499	109733	116455	125133	135477
LT2	104855	108899	116344	126344	138488	152555
LT3	82831	75723	73793	74967	78255	83137
LT4	78427	73165	73208	76550	82232	89750
LT5	82831	75723	73793	74967	78255	83137
LT6	78427	73165	73208	76550	82232	89750
LT7	69619	68050	72039	79716	90186	102988
LT8	104855	105499	109733	116455	125133	135477
LT9	104855	108899	116344	126344	138488	152555
LT10	78427	90144	106233	125955	148999	175155
LT11	82831	96098	113411	134255	158366	185622
LT12	69619	78237	91849	109366	130244	154222
LT13	82831	96098	113411	134255	158366	185622
LT14	78427	90144	106233	125955	148999	175155

Plate type	Aspect ratio					
	b/a					
	1	1.2	1.4	1.6	1.8	2
LT1	104855	75616	59355	49350	42740	38138
LT2	104855	73258	55986	45490	38620	33868
LT3	82831	66735	57864	52442	48878	46404
LT4	78427	62600	54196	49201	45984	43788
LT5	82831	66735	57864	52442	48878	46404
LT6	78427	62600	54196	49201	45984	43788
LT7	69619	54331	46862	42718	40198	38554
LT8	104855	75616	59355	49350	42740	38138
LT9	104855	73258	55986	45490	38620	33868
LT10	78427	50809	37351	29902	25380	22438
LT11	82831	52586	37649	29284	24153	20784
LT12	69619	47257	36755	31139	27835	25744
LT13	82831	52586	37649	29284	24153	20784
LT14	78427	50809	37351	29902	25380	22438

4. Conclusions

The main aim of this study was to calculate the critical buckling loads of quasi-isotropic rectangular plates so that a suitable lamination plan can be obtained at the preliminary structural design stage. It is pleasing for the authors to see that the findings of the study discussed in the previous section show that this aim is achieved.

Acknowledgments

The authors would like to thank Dr. Mark A. Gammon for his well appreciated help. The authors would like to dedicate this paper to Professor M. C. Dökmeci who made significant contribution to mechanics of composites.

References

- About.com Composites / Plastics (2013), <http://composite.about.com/library/data/blc-t300-934-1.htm> (Accessed on August 30, 2013)
- Altunsaray, E. and Bayer, İ. (2013), "Deflection and free vibration of symmetrically laminated quasi-isotropic thin rectangular plates for different boundary conditions", *Ocean Eng.*, **57**, 197-222.
- ASM Handbook (2001), *Volume 21, Composites*, ASM International.
- Baltaci, A., Sarikanat, M. and Yildiz, H. (2007), "Static stability of laminated composite circular plates with holes using shear deformation theory", *Finite Elem. Anal. Des.*, **43**(11-12), 839-846.
- Darvizeh, M. and Darvizeh, A. (2002), "Buckling analysis of composite plates using differential quadrature method (DQM)", *Steel Compos. Struct., Int. J.*, **2**(2), 99-112.
- Felix, D.H., Bambill, D.V. and Rossit, C.A. (2011), "A note on buckling and vibration of clamped orthotropic plates under in-plane loads", *Struct. Eng. Mech., Int. J.*, **39**(1), 115-123.
- Hu, H., Badir, A. and Abatan, A. (2003), "Buckling behavior of a graphite/epoxy composite plate under parabolic variation of axial loads", *Int. J. Mech. Sci.*, **45**(6-7), 1135-1147.
- Ides The Plastic Web (2013), <http://composites.ides.com> (Accessed on August 30, 2013)
- Mallik, P.K. (1997), *Composites Engineering Handbook*, Marcel Dekker Inc., NY, USA.
- Mouritz, A.P., Gellert, E., Burchill, P. and Challis, K. (2001), "Review of advanced composite structures for naval ships and submarines", *Comp. Struct.*, **53**(1), 21-41.
- Özben, T. (2009), "Analysis of critical buckling load of laminated composites plate with different boundary conditions using FEM and analytical methods", *Comp. Mat. Sci.*, **45**(4), 1006-1015.
- Panda, S.K. and Ramachandra, L.S. (2010), "Buckling of rectangular plates with various boundary conditions loaded by non-uniform inplane loads", *Int. J. Mech. Sci.*, **52**(6), 819-828.
- Powell, P.C. (1994), *Engineering with Fibre-Polymer Laminates*, Chapman & Hall, London, UK.
- Rajasekaran, S. and Wilson, A.J. (2013), "Buckling and vibration of rectangular plates of variable thickness with different end conditions by finite difference technique", *Struct. Eng. Mech., Int. J.*, **46**(2), 269-294.
- Reddy, J.N. (2004), *Mechanics of Laminated Composite Plates and Shells: Theory and Analysis*, (2nd Ed.), CRC Press, Boca Raton, FL, USA.
- Reuben, R.L. (1994), *Materials in Marine Technology*, Springer-Verlag London Ltd., UK.
- Saracoglu, M.H. and Özcelikörs, Y. (2011), "Tabakalı Kompozit Plakların Sonlu Farklar Yöntemi ile Statik Analizi", *Pamukkale Üniversitesi, Mühendislik Bilimleri Dergisi*, **17**(1), 51-62. [In Turkish]
- Shenoi, R.A. and Wellicome, J.F. (1993a), *Composite Materials in Maritime Structures, (Volume I Fundamental Aspects)*, Cambridge University Press, NY, USA.
- Shenoi, R.A. and Wellicome, J.F. (1993b), *Composite Materials in Maritime Structures, (Volume II Practical Considerations)*, Cambridge University Press, NY, USA.

Szilar, R. (2004), *Theories and Applications of Plate Analysis: Classical Numerical and Engineering Methods*, John Wiley & Sons, Inc., Hoboken, NJ, USA.

CC